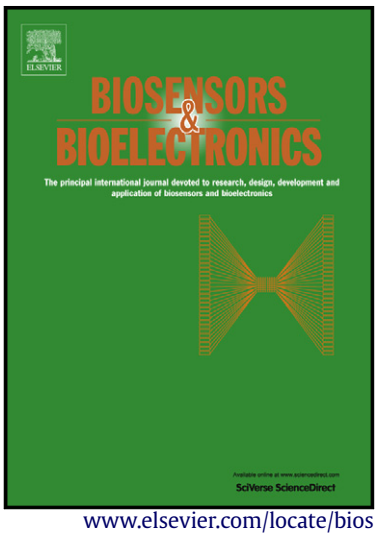

www.elsevier.com/locate/bios

A device design of an integrated CMOS poly-silicon biosensor-on-chip to enhance performance of biomolecular analytes in serum samples

Pei-WenYen , Che-WeiHuang , Yu-JieHuang , Min-ChengChen , Hsin-HaoLiao , Shey-ShiLu , Chih-TingLin

PII: S0956-5663(14)00342-X
DOI: http://dx.doi.org/10.1016/j.bios.2014.05.010
Reference: BIOS6771

To appear in: *Biosensors and Bioelectronics*

Cite this article as: Pei-WenYen , Che-WeiHuang , Yu-JieHuang , Min-ChengChen , Hsin-HaoLiao , Shey-ShiLu , Chih-TingLin , A device design of an integrated CMOS poly-silicon biosensor-on-chip to enhance performance of biomolecular analytes in serum samples, *Biosensors and Bioelectronics,* http://dx.doi.org/10.1016/j.bios.2014.05.010

A device design of an integrated CMOS poly-silicon biosensor-on-chip to enhance performance of biomolecular analytes in serum samples

Pei-Wen Yen[1], Che-Wei Huang[2], Yu-Jie Huang[2], Min-Cheng Chen[3], Hsin-Hao Liao[4], Shey-Shi Lu[2], and Chih-Ting Lin[1,2,*]

[1]Graduate Institute of Biomedical Electronics and Bioinformatics, National Taiwan University, Taipei, Taiwan

[2] Graduate Institute of Electronics Engineering, National Taiwan University, Taipei, Taiwan

[3]National Nano Device Laboratory, National Applied Research Laboratories, Hsinchu, Taiwan

[4]National Chip Implementation Center, National Applied Research Laboratories, Hsinchu, Taiwan

*Corresponding author. Tel: +886 2 33669603, Fax: +886 2 23681679 Email: timlin@ntu.edu.tw

Abstract

For on-site clinical diagnosis of biomolecules, the detection performances of most point-of-care (POC) biosensor devices are limited by undesired cross-detection of other non-analyte proteins in patient serum samples and other complex samples. To conquer this obstacle, this work presents a fully integrated bottom-gate poly-silcion nanowire (polySi NW) biosensor system-on-chip (SoC) to enhance the detection performance of cardiac-specific troponin-I (cTnI) concentration levels in serum samples. By applying proper electrical potential at the bottom gate under polySi NW biosensor, the biosensor response to cTnI biomarker can be improved by at least 16 fold in 50% phantom serum samples. The experimental result shows its detection range is from 3.2×10^{-13} M(mol.l^{-1}) to 3.2×10^{-10} M. This enhancement can be attributed to the electrostatic interactions between target biomolecules and voltage-applied bottom gate electrodes. This is the first time that a polySi NW CMOS biosensor chip has shown feasibilities to detect specific biomarkers in serum samples. Therefore, the developed technology paves the way toward on-field applications of CMOS compatible SiNW biosensing technologies and it can be employed for future biomolecular analysis in on-site serum diagnosis applications.

Keywords

Poly-silicon nanowire, biosensor, Electrical protein manipulating, biomolecular analytes in serum samples

1. Introduction

The blood serum test is an essential and indispensible laboratory technique for clinical medical diagnosis. Within serum, the concentration level of crucial biomarkers is important to evaluate the health conditions of patients (Toner and Irimia 2005). In traditional serum tests, well-trained technicians and sophisticated instruments are required with a long analysis time in a central lab. As a consequence, traditional serum tests are time-consuming, labor-intensive, and cost-ineffective. These drawbacks lead to inconveniences for patients who should be monitored frequently and for

clinics with limited resources (Mabey et al. 2004). Therefore, there are increasing demands for biomarker sensing technologies for on-site serum diagnosis. These demands promote the development of point-of-care biosensing devices (Moore 2013).

Among various POC biomarker-sensing technologies, the CMOS compatible technique is promising because of its characteristics, e.g. cost-effective fabrication, miniaturization, and ease of integration (Adiguzel and Kulah 2012). As a consequence, different types of CMOS-compatible ultrasensitive biosensors have been reported and investigated, such as microcantilevers (Huang et al. 2013a), ion-sensitive field-effect transistors (Seong-Jin and Euisik 2012) and nanowires (Chen et al. 2011). Among these biosensing technologies, the silicon nanowire (SiNW) field-effect sensor has attracted substantial attentions because of its ultra-high sensitivity for different biological molecules, such as viruses, DNA/miRNA, proteins, and antibodies (He et al. 2008; Patolsky et al. 2007; Patolsky et al. 2004; Stern et al. 2007; Stern et al. 2010). In previous works, most of the ultra-high detection capabilities of SiNWs are demonstrated in prepared buffer solutions with complicated purification procedures. To function as an on-site serum diagnosis device, however, interferences from abundant non-analyte background proteins should be taken into consideration. Therefore, it is necessary to enhance signals from biomarker recognition and increase probabilities of bio-recognition activities for clinical serum tests.

Previously, several studies have reported that manipulations of charged biomolecules can be achieved by changing electrostatic polarity on solid surfaces. This manipulation can be accomplished by applying external potential and increasing the biomolecular adsorption onto solid surfaces (Brusatori and Van Tassel 2003; Song et al. 2008; Yen et al. 2009). In this work, this concept is employed to enhance the probability of biomarker binding for biomarker detection in serum samples. To accomplish the proposed method, we presents the design of a bottom-gate poly-SiNW biosensor system-on-chip (BG-bioSSoC), which can be implemented by a standard CMOS process. To evaluate BG-bioSSoC performance in serum samples, human cTnI is chosen as the detection target. The concentration levels of cTnI (<0.4 ng/mL at normal status) are dramatically elevated nearly 10 folds in patient blood streams after the onset of a fatal acute myocardiac infarction (AMI) (Wu et al. 1999). It can be used as a long-term prognostic factor for an acute coronary syndrome patient (Ohman et al. 1996). From BG-bioSSoC experimental results, the cTnI detection in serum background can be significantly enhanced with the bottom gate design even if this detection suffers from backgroun-protein interferences. For the first time, the bottom-gate design with a fully integrated CMOS biosensing SoC shows feasibilities of biomarker detections in serum samples. This demonstrates a potential to perform a robust POC device for personalized biomarker diagnosis in an on-site blood serum test.

2. Materials and methods

2.1 Chemical reagents and biomarkers

Chemicals used in the protocol of cTnI detection experiments, such as Bovin serum albumin (BSA), Phosphate buffer saline (PBS), (3-Aminopropyl)triethoxysilane (≥98%, APTES), and

Glutaraldehyde solution (~50% in H_2O, GA), were purchased from Sigma-Aldrich (St. Louis, USA). The used APTES solution was diluted with 99% ethanol and the BSA solution was diluted with PBS buffer to the final concentration respectively. On the other hand, the biomarkers, cTnI and anti-cTnI polyclonal antibody, were purchased from AbCam (Cambridge, UK). The Fetal bovin serum (FBS), purchased from Invitrogen, was used as the phantom serum with total protein concentration approximately 42mg/ml. The FBS sample was diluted with PBS buffer to 50% v/v ratio for experiments. Furthermore, in this paper, PBS (10 mM phosphate, pH 7.4) was diluted to 0.01X and introduced as measurement buffer solution in the measuring step. Under this dilution ratio, the ionic strength is 1.8mM and Debye length is ~7.3nm of the PBS buffer respectively. (Chua et al. 2009) All biomarkers and serum samples were stored at -20℃ before use.

2.2 Design and implementation of BG-bioSSoC

The biomolecular sensing of a SiNW biosensor is based on the binding of charged biomoelcules (Kong et al. 2012). The charged biomolecules in a buffer solution can be coupled with appropriate functionalized SiNWs by antibody-antigen bindings. These biomolecules bounded on the SiNW surface induce the redistribution of SiNW carriers and modulate the SiNW conduction channel. As a consequence, the conductance of the SiNW channel changes with the number of binding biomolecules. To improve the sensing response of a SiNW biosensor, different SiNW fabrication parameters, e.g. size and doping, have been discussed (Li et al. 2011). However, these parameters are strictly constrained in standard CMOS foundries, which manufacture devices for real applications. Without changing preset conditions of standard CMOS processes, it is intriguing to exploit the nature of biomolecules to enhance SiNW biosensing responses. Because biomolecules are naturally charged in solutions, their local concentrations near the SiNW surface can be increased by applying external electrical fields. This concentration enhancement can promote the binding probability between targeted biomolecules and the functionalized SiNW biosensor. On the basis of this design concept, a bottom-gate structure is designed and implemented to enhance the detection capability of SiNWs for serum sample diagnosis.

To implement the proposed BG-bioSSoC design, a 0.35 μm 2P4M CMOS commercially-available standard fabrication process has been chosen. The standard content layers of 0.35μm fabrication process are shown in Fig. S1†. In this standard commercial process, there are two polySi layers, i.e., one with degenerated doping (N^+ doping) for the polySi gate (N^+Poly1) and the other lightly doped (N^+ doping) for on-chip resistors (N^+Poly2). Because the sensitivity of SiNWs improves with a low doping concentration (Li et al. 2011; Nair and Alam 2007), the lightly doped layer is chosen to be a poly-SiNW biosensor and the degenerated doping layer is used as a bottom-gate structure for applied bottom-gate voltage(V_{bottom}) application. The schematic of this novel bottom-gate poly-SiNW biosensor is shown in Fig. 1(a). To control the external electrical field around the poly-SiNW, in this device design, the bottom-gate layer (N^+Poly1) is beneath the poly-SiNW (N^+Poly2) sensing film. This architecture can avoid the

interference of circuit operations while the external electrical field is applied. The cross-section image of the fabricated bottom-gate poly-SiNW device along the dash line axis from Fig. 1(a) is shown in Fig. 1(b). The height and width of the poly-SiNW are 167 nm and 625 nm, respectively. The oxide thickness between the poly-SiNW and the bottom-gate layer is 120 nm.

Figure 1

Because the poly-SiNW biosensor can be modeled as a resistance in circuits, a classical Wheatstone full bridge interface architecture, as shown in Fig. 2(a), is used to minimize environmental noises and process variations. In the Wheatstone bridge architecture, the top oxide layer (TEOS) of the two poly-SiNW biosensors was opened by a post fabrication process, i.e. R1 and R4 ,whereas the TEOS of the other two reference poly-SiNW biosensors was kept intact. The TEOS post fabrication process was reported in our previous work (Huang et al. 2013b). In brief, the top passivation layer (Si_3N_4) in the sensing region was removed in standard CMOS processes. The exposed TEOS in the sensing region was etched by reactive ion etching (RIE) and buffer hydrofluoric acid (BHF) processes respectively. This post-etching process reduces TEOS thickness on the top of the poly-SiNW biosensors. The implemented BG-bioSSoC and the sensing environmental setup system are shown in Fig. 2(b). The red square line represented the BG-bioSSoC chip with epoxy passivation for the pad region. This passivation was performed with epoxy covering, and a plastic reservoir was used to retain aqueous samples with BG-bioSSoC (Huang et al. 2013b). With a perfect epoxy protection, the entire chip could be operated in a liquid sensing environment without a short circuit effect. To harness the advantages of CMOS integrated circuits, the developed BG-bioSSoC integrates a set of bottom-gate poly-SiNW biosensors, a low-noise analog front-end (AFE), a 10-bit analog-to-digital converter (ADC), a microcontroller, and an on-off-key (OOK) wireless transceiver. It should be noted that the temperature effect from the Wheatstone bridge architecture can be compensated by an on-chip junction-based CMOS temperature sensor.

Figure 2

2.3 Surface functionalization of poly-SiNW

It is necessary to functionalize the surface of poly-SiNW to have the ability to detect cTnI. The surface immobilization procedures to functionalize the poly-SiNW biosensor can be briefly described as follows: (1) After the post etching fabrication process, the BG-bioSSoC chip was directly immersed in the 2% APTES solution for 1 hour for silanization. After being washed with ethanol several times, the chip was baked in 95 °C for 15 min. (2) The chip was immersed in the 2.5% GA for 1 hour and then washed with deionized (DI) water several times. GA can interact

with the amine group of APTES to form a cross-linked functional group; (3) Following previous crosslink procedures, the anti-cTnI antibody was dripped on the chip surface in a humidity chamber at 4 °C overnight. (4) After the anti-cTnI antibody immobilization process, the chip was washed by PBS buffer and immersed in 1% BSA solution to block uncross-linked GA. Then, the chip was rinsed with PBS buffer three times and was ready for measurements.

2.4 Experimental protocol and measurement setup

To examine the implemented BG-bioSSoC, the plastic reservoir and epoxy passivation of the chip circuit interconnections is necessary for operating under a liquid environment. In our experiment, all of the liquid samples were nearly 150 μl in volume, and the liquid was exchanged by pipetting. This liquid volume is sufficient to cover the entire surface of BG-bioSSoC. Because of the limited quantities of BG-bioSSoCs, it should be noted that each experimental point was measured from 3 independent chips, i.e. N = 3. The measurement procedures of cTnI target protein in phantom serum, i.e. 50% FBS, are described as follows: (1) The initial background level is first measured in the measurement buffer, 0.01X PBS, via a functionalized BG-bioSSoC device nearly 15 min without applying a V_{bottom}. (2) Following the initialization, the cTnI target proteins of different concentrations are mixed in background interference buffers, i.e., phantom serums, and dripped in the reservoir for a target protein binding process. (3) During the biomolecular (antigen-antibody) binding process, varying values of V_{bottom} were applied the BG-bioSSoC with for nearly 15 min. (4) After the bimolecular binding process, the applied V_{bottom} was removed. (5) In the measurement step, the mixed sample solutions were rinsed off three times with measurement buffer and measured for 10 mins. For the experiment of the cTnI target protein in 0.5mg/ml BSA as phantom samples, the measurement procedures are the same as described in the aforementioned steps.

The measurement results are the AFE output voltage difference of the BG-bioSSoC obtained from the measurement step and initialization step. Moreover, the measurement results of the cTnI target protein in the phantom sample can be represented as a normalized detection response (NDR), which is defined as:

$$\mathrm{NDR}\left(\Delta V / V_0\right) = \left(V_S - V_0\right) / V_0 \ , \qquad (1)$$

where V_S is the AFE output voltage, which is detected in the measurement buffer after the biomolecular binding process under phantom samples containing cTnI with different concentrations, and V_0 is the AFE output voltage obtained from the initial background level in the measurement buffer.

3. Results and discussion

3.1 BG-bioSSoC experimental results

3.1.1 BG-bioSSoC pH validation

It is important to validate the implemented BG-bioSSoC by pH measurement because the unfunctionalized poly-SiNW biosensor can be characterized as a hydrogen ion sensor. With

protonation and deprotonation of the poly-SiNW surface in different standard pH buffers, the carrier distribution within poly-SiNW can be modulated. To experimentally validate the BG-bioSSoC in buffers with different pH values, the AFE output voltage was recorded for 50 seconds for each pH value. As shown in Fig. 3(a), the AFE output of BG-bioSSoC is decreased from pH 9 to pH 5 because of the increase in the number of protons on the n-type poly-SiNW surface. This experimental result is similar to previous reported work (Simon M. Sze 2006). In Fig. 3(a), the pH response of the implemented n-type poly-SiNW device at the condition of pH>7 (i.e., pH ~9 to pH ~7) is more than that at the condition of pH<7 (i.e., pH ~7 to pH ~5). This shows that the implemented n-type poly-SiNW is more sensitive to negatively charged species. Furthermore, similar to most silicon based FET biosensors, the BG-bioSSoC is both pH and ion concentration dependence. To minimize the signal variations, the ion concentration and pH value of the measurement buffer are strictly controlled by the 0.01X PBS buffer (0.1mM phosphate, pH 7.4).

3.1.2 The interference by non-analyte background proteins

To demonstrate the capabilities of the developed biosensors, the most concerning point is the interference by non-analyte background proteins which represents biomolecules different from the target analyte in buffers or bio-samples. This interference results from nonspecific adsorption and binding of background proteins onto the developed biosensor surfaces. As a consequence, it is important to evaluate the detection signals of BG-bioSSoC degradation caused by background proteins in prepared testing samples. For this evaluation, cTnI was chosen as the detection target. The charge of the cTnI target protein is related to its own isoelectric point (pI) values and the pH value of the measurement buffer (0.01X PBS, pH 7.4). According to previous reports, the pI value of cTnI is generally 5.2–5.4. (Lee et al. 2012) The cTnI has negative charges in the measurement buffer because of pI values lower than pH 7.4. Based on our biosensing experiments, the cTnI target protein is predicted to have negative charges, resulting in a carrier redistribution of n-type poly-SiNW and consequently a change in the conductance. To have detection specificity for cTnI, as in the aforementioned protocols, the poly-SiNW device was washed with DI and immobilized with anti-cTnI antibody. For the testing sample imitated biological samples, on the other hand, bovine serum albumin (BSA) and fetal bovine serum (FBS) were used to demonstrate the interference effect. Fig. 3(b) shows the BG-bioSSoC biosensing results of cTnI in 0.5 mg/ml BSA background (compared with 0.35 mg/100 ml in whole blood) and 50% FBS background solutions. To evaluate the sensing result, $NDR_{in\ BSA}$ and $NDR_{in\ FBS}$ are set as the difference in BG-bioSSoC obtained from cTnI binding conditions under phantom samples of 0.5 mg/ml BSA and 50% FBS, as shown in Fig. 3(b). From this experimental result, the NDR ratio, i.e., $(NDR_{in\ BSA} / NDR_{in\ FBS})$, is 0.025/0.011 with a cTnI concentration of 3.2×10^{-10} M. This shows that the NDR deterioration is nearly double with complicated background, i.e., 50% FBS, compared with a simple background, i.e., 0.5 mg/ml BSA. This results from the existing contents, e.g., electrolytes, antigens, hormones and etc., in FBS serums. As a consequence, it is important to improve the

BG-bioSSoC detection capabilities under severe interferences from background proteins.

Figure 3

3.2 The improvement from employing bottom electrical potential

To improve the BG-bioSSoC detection capability under background interference, an external electrical field is introduced by the bottom-gate design. This bottom-gate electrical field manipulation of proteins in solution can be achieved by electrostatic interactions with charged group of proteins. To prevent electrolysis in ionic buffer solutions while applying a bottom-gate electrical field, the bottom-gate electrode is covered with a top oxide layer (Fig. 1(b)). In experiments, this bottom-gate electrical field was applied with positive voltage because of constrains on the voltage tolerance of the 0.35□μm CMOS standard process. As mentioned above in the experimental protocols, it should be noted that the V_{bottom} was only applied in incubation steps rather than in measurement steps. The experimental results are shown in Fig. 4(a) and expressed with NDR performance with different values of V_{Bottom} applied in 50% FBS phantom samples. As the concentration of cTnI is 3.2×10^{-11} M, shown in Fig. 4(a), the NDR improvement ratio of 0.5 V_{Bottom} / 0 V_{Bottom} is 1.3 (1.26×10^{-2} / 9.43×10^{-3}) and 1 V_{Bottom} / 0 V_{Bottom} is 16.5 (1.56×10^{-1} / 9.43×10^{-3}). This detection enhancement might be a result of electrostatic interactions between negatively charged cTnI and the positive potential of the bottom gate. Because negatively charged cTnI molecules are attracted toward the surface, this electrostatic interaction can increase the probability of antibody-antigen binding events. Although this enhancement mechanism is also subject to interference by background proteins in 50% FBS samples, the binding affinity to anti-cTnI antibodies of those non-specific binding biomolecules is significantly less than that of cTnI molecules. With competitive-binding processes, as a consequence, the bounded chance of non-specific biomolecules is less than that of cTnI. At the same time, the number of cTnI molecules near the poly-SiNW biosensor surface can be increased by the electrostatic interaction. This further enhances the binding probability of cTnI and the detection response of poly-SiNW biosensing devices. In Fig. 4(a), the detection improvement can be clearly demonstrated by comparing the fitted curve of 0 V_{Bottom} and 1 V_{Bottom}. The logarithmic dependence of the sensor response to cTnI concentration can be supported by previous works, such as a theoretical simulation suggested that the nonlinear screening effect by electrolytes results in the logarithmic sensor response (Nair and Alam, 2008) and an experimental result also showed a logarithmic dependence of nanowire biosensor responses to the target protein concentration (Gao et al., 2011). In addition, with applying the different values of V_{bottom} over 0.75V, the detection range of cTnI concentration levels can be identified from 3.2×10^{-13} M (7.6 pg/ml) to 3.2×10^{-10} M (7.6 ng/ml). This detection range (7.6 pg/ml~7.6 ng/ml) is hardly achieved without applying the external electrical field. Moreover, this detection sensitivity of cTnI concentration by BG-bioSSoC is nearly two orders of magnitude better than that (1ng/ml) detected by the enzyme-linked immunosorbent assay (ELSIA).

By increasing the bottom-gate electrical potential to more than 1 V, this signal-enhancement

phenomenon deteriorates significantly as shown in Fig. 4(b). This figure shows that the NDR of 1.5 V_{Bottom} is worse than that of 0 V_{Bottom}, a state in which no bottom-gate voltage is applied. This illustrates that other factors should be addressed while applying a V_{bottom} in BG-bioSSoC devices. Given previous studies, there are two possible factors affecting NDR under high electrical fields. One possible factor is that the high electrical field might cause a deformation of protein secondary structures (Song et al. 2008). In addition, it is reported that the low external electrical field also causes a change in protein conformation due to the perturbation of hydrogen-bond stability (Innocent et al. 2014). Both of these effects decrease the binding affinity between antigen-antibody conjugates and result in the decrease of NDR. Another possible factor is the charging effect within the interfaces of the oxide. With an applied electrical field, carriers can easily be trapped in dielectrics through oxygen-related defect traps (Hair and Tripp 1995; Tripp and Hair 1992). This charge trapping mechanism mainly occurs at the silicon-oxide interface and near the surface-silanol groups, which are easily charged (Kim et al. 2003; Paska and Haick 2012). Moreover, it is also reported that the charge trapping effect occurs under the application of an external electrical field in a dielectric film (Katz et al. 2002; Yamin 1965; Li et al. 2008). Under high electrical fields, as a consequence, charges are easily injected into the dielectric trapping center from the liquid- solid oxide surface on the top of the poly-SiNW. These trapped charges result in a serious charging effect on poly-SiNW biosensing devices. To verify the proposed trapping effect, Fig. 4(c) shows experimental results of pH measurements in PBS buffer with different applied V_{bottom} by unfunctionalized BG-bioSSoC. In these experiments, the NDR_{pH}, can be defined as:

$$\mathrm{NDR}_{pH}\left(\Delta V_{pH} / V_{pH\sim5}\right) = \left(V_{pH} - V_{pH\sim5}\right) / V_{pH\sim5} \quad , \qquad (2)$$

where V_{pH} is the AFE output voltage that is detected in the different standard pH buffers, and $V_{pH\sim5}$ is the AFE output voltage obtained from the pH ~5 buffer. Both output signals are measured and normalized under certain V_{bottom} value respectively.

Figure 4

Given Fig. 4(c), it is clear that the NDR_{pH} signal degradation effect can be clearly observed by applying V_{bottom}. Based on previous works (Cheng et al., 2008), it was suggested that the effect of charges trapping/detrapping in the dielectric results in this phenomenon. This effect shows an exponential dependence of the applied voltage on nanowire FET devices. It is clear that this charging effect suppresses the sensor response related to antigen- antibody binding events. As a consequence, the combination of these two factors, protein deformation and surface charging, lead to a seriously decreased NDR of a poly-SiNW biosensor under high applied V_{bottom}, e.g. V_{Bottom} = 1.5 V.

Figure 5

To demonstrate the NDR enhancement introduced by different applied values of V_{bottom}, the experimental results of cTnI in 50% FBS serum solutions with different values of V_{Bottom} can be shown in Fig. 5. Here, the NDR enhancement is defined as follows:

$$\text{NDR enhancement} = \text{NDR (with } V_{Bottom}\text{)/NDR (without } V_{Bottom}\text{).} \quad (3)$$

In Fig. 5, the black arrow pointing the left direction of 1 V_{bottom} is the NDR- improved region and the other direction is the NDR- degraded region. The maximum NDR enhanced ratio is 16.5/1 at V_{Bottom} = 1 V with cTnI concentration at 3.2×10^{-11} M. At V_{Bottom} = 1.5 V, however, the NDR enhanced ratio is reduced to 0.6/1 with cTnI concentration at 3.2×10^{-11} M. As mentioned above, the deterioration in NDR enhancement results from the competing effects between the improved factor, i.e. electrostatic force, and the degraded factors, i.e. protein deformation and surface charging effect. Therefore, the response of a poly-SiNW biosensor in serum samples can be improved with proper applied V_{bottom}, e.g. within 1 V.

Table 1

On the other hand, from table 1, it should be noted that the V_{Bottom} enhancement effect is more significant in low cTnI concentration, e.g. 3.2×10^{-12} M, than in high cTnI concentration, e.g. 3.2×10^{-11} M. This can contribute to the saturation of antibody binding sites on the sensor surface. In summary, the developed BG-bioSSoC has a cTnI limit-of-detection at 7.6 pg/ml in a 50% FBS phantom sample by manipulating V_{Bottom} to enhance the response of the biosensors. This demonstrates the potential of BG-bioSSoC for biomoelcular diagnosis in serum samples.

4. Conclusions

This work presents a fully integrated BG-bioSSoC for cTnI detection in 50% FBS serum samples. The developed BG-bioSSoC is implemented by a 0.35 μm 2P4M CMOS commercial-available standard fabrication process that is compatible with mass-production. By applying a proper V_{Bottom} to a functionalized BG-bioSSoC, the sensor response of cTnI detection in 50% FBS serum samples can be improved by a factor of 16, and the detection sensitivity of BG-bioSSoC is nearly two order magnitudes better than that of ELISA based assay. The results in this work suggest that this BG-bioSSoC with proper V_{Bottom} has potential to be implemented as a POC device for fast clinical diagnosis applications. For instance of this application, with a statistic BG-bioSSoC device pre-calibration, the cTnI concentration level threshold is set to indicate whether the patient has a high risk of onset of AMI or coronary syndrome. For the first time, the bottom-gate design with a fully integrated CMOS biosensing SoC shows feasibilities for biomolecular analyte detection in serum samples. This work makes advances toward on-field applications of CMOS compatible SiNW biosensing technologies.

Acknowledgements

The authors would like to thank the financial supporting from National Science Council (NSC) in

Taiwan (101-2220-E-002-021, 102-2220-E-002-009, and 101-2628-E-001-002-MY3) and National Taiwan University (103R890941).

Reference

Adiguzel, Y., Kulah, H., 2012. Sensors 12, 10042-10066.

Brusatori, M.A., Van Tassel, P.R., 2003. Biosens. Bioelectron. 18, 1269-1277.

Chen, K.I., Li, B.R., Chen, Y.T., 2011. Nano Today 6, 131-154.

Cheng, Y., Xiong, P., Yun, C.S., Strouse, G.F., Zheng, J.P., Yang, R.S., Wang, Z.L., 2008. Nano Lett. 8, 4179-4184.

Chua, J.H., Chee, R.E., Agarwal, A., Wong, S.M., Zhang, G.J., 2009. Anal. Chem. 81, 6266-6271.

Gao, A.R., Lu, N., Dai, P.F., Li, T., Pei, H., Gao, X.L., Gong, Y.B., Wang, Y.L., Fan, C.H., 2011. Nano Lett. 11, 3974–3978.

Hair, M.L., Tripp, C.P., 1995. Colloids Surf., A. 105, 95-103.

He, B., Morrow, T.J., Keating, C.D., 2008. Curr. Opin. Chem. Biol. 12, 522-528.

Huang, C.W., Hsueh, H.T., Huang, Y.J., Liao, H.H., Tsai, H.H., Juang, Y.Z., Lin, T.H., Lu, S.S., Lin, C.T., 2013a. Sens. Actuator B-Chem. 181, 867-873.

Huang, C.W., Huang, Y.J., Yen, P.W., Tsai, H.H., Liao, H.H., Juang, Y.Z., Lu, S.S., Lin, C.T., 2013b. Lab. Chip. 13, 4451-4459.

Innocent, B., Dave, E.D., 2014. Soft Matter. 10, 431-437.

Katz, H.E., Hong, X.M., Dodabalapur, A., Sarpeshkar, R., 2002. J. Appl. Phys. 91, 1572-1576.

Kim, W., Javey, A., Vermesh, O., Wang, O., Li, Y.M., Dai, H.J., 2003. Nano. Lett. 3, 193-198.

Kong, T., Su, R., Zhang, B., Zhang, Q., Cheng, G., 2012. Biosens. Bioelectron. 34, 267-272.

Lee, I., Luo, X., Huang, J., Cui, X.T., Yun, M., 2012. Biosensors. Biosensors. 2, 205-220.

Li, H., Zhang, Q., Marzari, N., 2008. Nanotechnology 19, 175203.

Li, J., Zhang, Y., To, S., You, L., Sun, Y., 2011. ACS. Nano. 5, 6661-6668.

Mabey, D., Peeling, R.W., Ustianowski, A., Perkins, M.D., 2004. Nat. Rev. Microbiol. 2, 231-240.

Moore, C., 2013. J. Hosp. Infect. 85, 1-7.

Nair, P.R., Alam, M.A., 2007. IEEE. T. Electron. Dev. 54, 3400-3408.

Nair, P.R., Alam, M.A., 2008. Nano. Lett. 8, 1281-1285.

Ohman, E.M., Armstrong, P.W., Christenson, R.H., Granger, C.B., Katus, H.A., Hamm, C.W., O'Hanesian, M.A., Wagner, G.S., Kleiman, N.S., Harrell, F.E., Jr., Califf, R.M., Topol, E.J., 1996. N. Engl. J. of med. 335, 1333-1341.

Paska, Y., Haick, H., 2012. ACS. Appl. Mater. Interfaces. 4, 2604-2617.

Patolsky, F., Timko, B.P., Zheng, G.F., Lieber, C.M., 2007. Mrs. Bull. 32, 142-149.

Patolsky, F., Zheng, G., Hayden, O., Lakadamyali, M., Zhuang, X., Lieber, C.M., 2004. Proc. Natl. Acad. Sci. U. S. A. 101, 14017-14022.

Seong-Jin, K., Euisik, Y., 2012. IEEE. Trans. Biomed. Circuits Syst. 6, 189-196.

Simon M. Sze, K.K.N., 2006. Physics of Semiconductor Devices, 2nd ed. John Wiley & Sons, New

York.

Song, Y.Y., Li, Y., Yang, C., Xia, X.H., 2008. Anal. Bioanal. Chem. 390, 333-341.

Stern, E., Klemic, J.F., Routenberg, D.A., Wyrembak, P.N., Turner-Evans, D.B., Hamilton, A.D., LaVan, D.A., Fahmy, T.M., Reed, M.A., 2007. Nature. 445, 519-522.

Stern, E., Vacic, A., Li, C., Ishikawa, F.N., Zhou, C., Reed, M.A., Fahmy, T.M., 2010. Small. 6, 232-238.

Toner, M., Irimia, D., 2005. Annu. Rev. Biomed. Eng. 7, 77-103.

Tripp, C.P., Hair, M.L., 1992a. Langmuir. 8, 1120-1126.

Tripp, C.P., Hair, M.L., 1992b. Langmuir. 8, 1961-1967.

Wu, A.H.B., Apple, F.S., Gibler, W.B., Jesse, R.L., Warshaw, M.M., Valdes, R., 1999. Clin. Chem. 45, 1104-1121.

Yamin, M., 1965. IEEE. T. Electron. Dev. 12, 88-96.

Yen, Y.K., Huang, C.Y., Chen, C.H., Hung, C.M., Wu, K.C., Lee, C.K., Chang, J.S., Lin, S.M., Huang, L.S., 2009. Sens. Actuator B-Chem. 141, 498-505.

Figure legends

Figure 1 (a) Schematic illustrates a novel bottom gate poly-SiNW biosensor design. The poly-SiNW and bottom gate are fabricated by N+ poly 2 layer and N+ poly 1 layer respectively. The dash-line represented the cross-section view of Fig. 1(b). (b) A cross-section SEM image of fabricated novel bottom gate poly-SiNW biosensor. The cross-section is generated by Focus Ion Beam (FIB). Where field Ox represents as the field oxide layer in 0.35 μm commercial-available standard CMOS process.

Figure 2 (a) Schematic illustrates n-type poly-SiNWs biomolecular senseing mechanism through Wheatstone bridge architecture. As the biomolecules bind to the functionalized SiNWs surface, the SiNWs carrier redistribution results in the resistance changes and the Wheatstone output voltage also changes. (b) The image of the fabricated BG-bioSSoC with labeled functional blocks and the sensing environmental setup system.

Figure 3 (a) An experimental result of the fabricated BG-bioSSoC device is validated by pH value measurement. (b) An experimental result of the functionalized BG-bioSSoC device measuring cTnI with background interferences, i.e., 0.5 mg/ml BSA and 50% FBS respectively.

Figure 4 The experimental results of the functionalized BG-bioSSoC device measuring cTnI in 50% FBS phantom samples with different V_{Bottom} applied during antigen-antibody binding state. (a) The NDR measurement result of applying varying values of V_{Bottom} below 1 V with the logarithm fit curve of 0 V_{Bottom} and 1 V_{Bottom} represent respectively. (b) The NDR measurement result of applying varying values of V_{Bottom} from 1 V to 1.5 V with the logarithm fit curve of 0 V_{Bottom} and 1.5 V_{Bottom} represent

respectively. The NDR result of applying 0 V_{Bottom} is also shown in the same graph. (c) An experimental result of series pH measurements with applying varying values of V_{Bottom} to verify the BG-bioSSoC trapping effect.

Figure 5 The experimental result of NDR enhancement measured of varying cTnI concentration (C_{cTnI}) in 50% FBS serum under different applied V_{Bottom}. The maximum NDR enhancement is observed under V_{Bottom} applied 1V. The black arrow pointing the left direction of 1 V_{bottom} is the NDR- improved region and the other direction is the NDR- degraded region.

Table 1 The NDR enhancement result measured with varying cTnI concentration (C_{cTnI}) in 50% FBS serum under different applied V_{Bottom}. The enhancement effect is more significant in low cTnI concentration, i.e., 3.2pM, than high concentration. The standard Deviation (SD) is also shown in the same table.

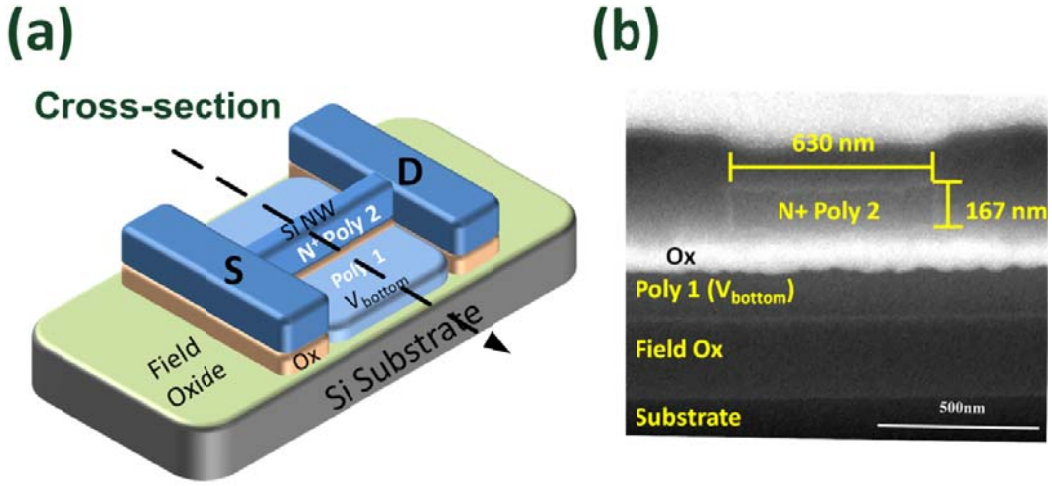
(a)
Cross-section
D
S
Si NW
N+ Poly 2
Poly 1
V bottom
Field Oxide
Ox
Si Substrate
(b)
630 nm
N+ Poly 2
167 nm
Ox
Poly 1 (V bottom)
Field Ox
Substrate
500nm

Fig . 1

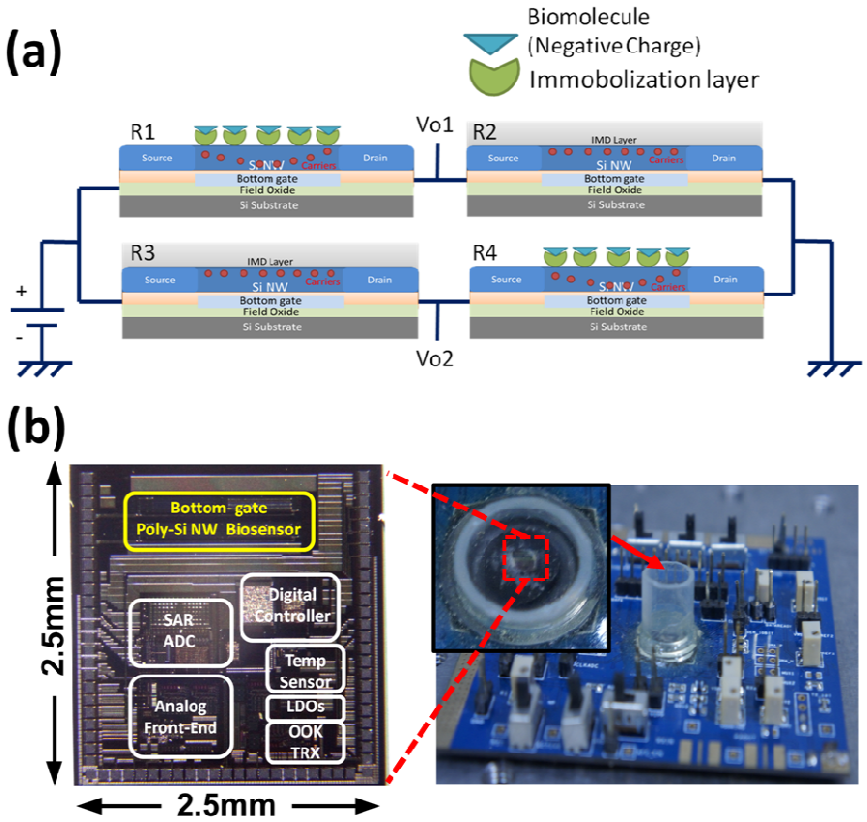
(a)
Biomolecule
(Negative Charge)
Immobolization layer
R1
R2
R3
R4
Vo1
Vo2
Source
Drain
Si NW
Carriers
IMD Layer
Bottom gate
Field Oxide
Si Substrate
+
-
(b)
Bottom-gate
Poly-Si NW Biosensor
Digital Controller
SAR ADC
Temp Sensor
Analog Front-End
LDOs
OOK TRX
2.5mm
2.5mm

Fig. 2

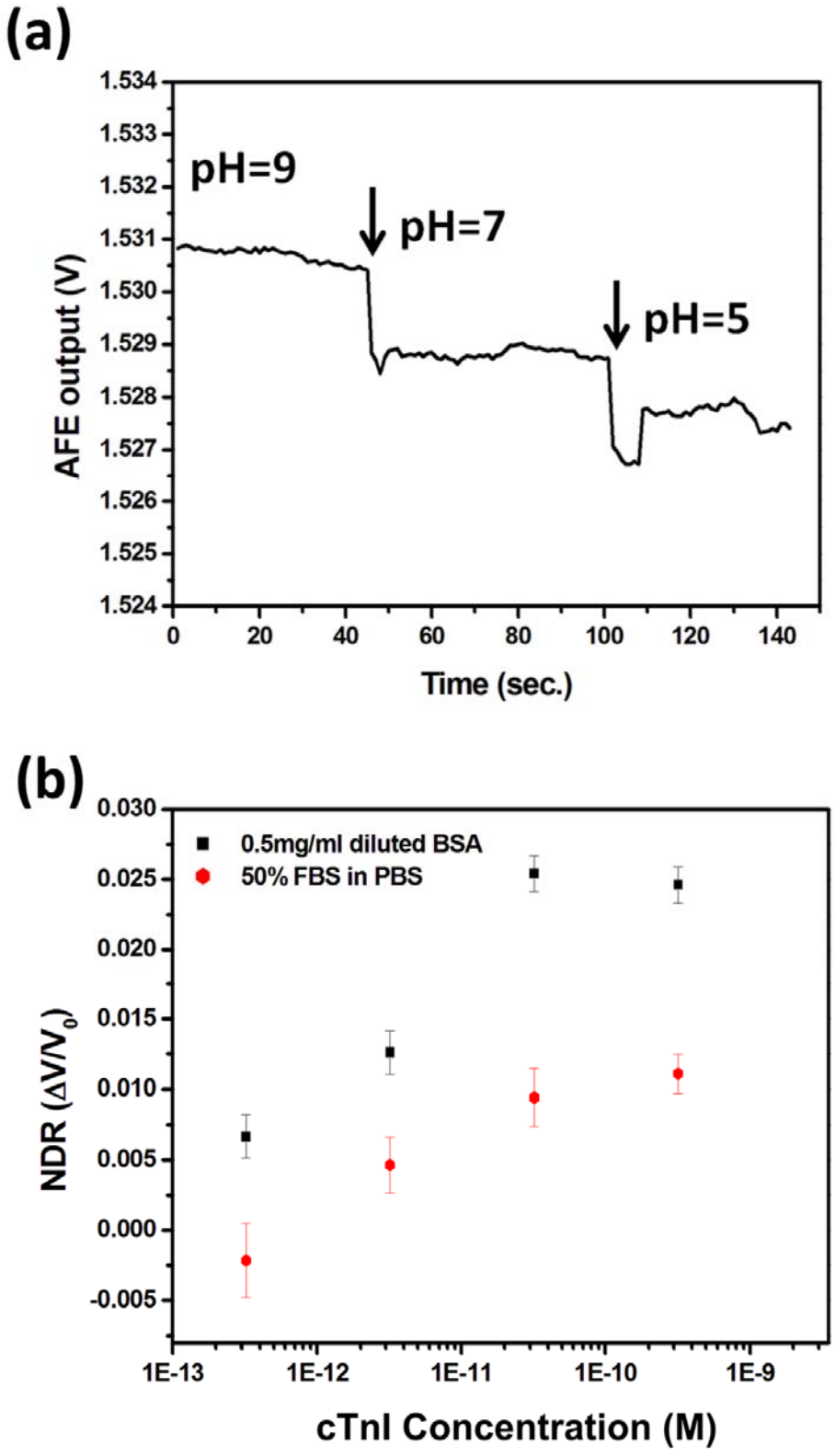
(a)
pH=9
pH=7
pH=5
AFE output (V)
Time (sec.)
(b)
0.5mg/ml diluted BSA
50% FBS in PBS
NDR (ΔV/V0)
cTnI Concentration (M)

Fig. 3

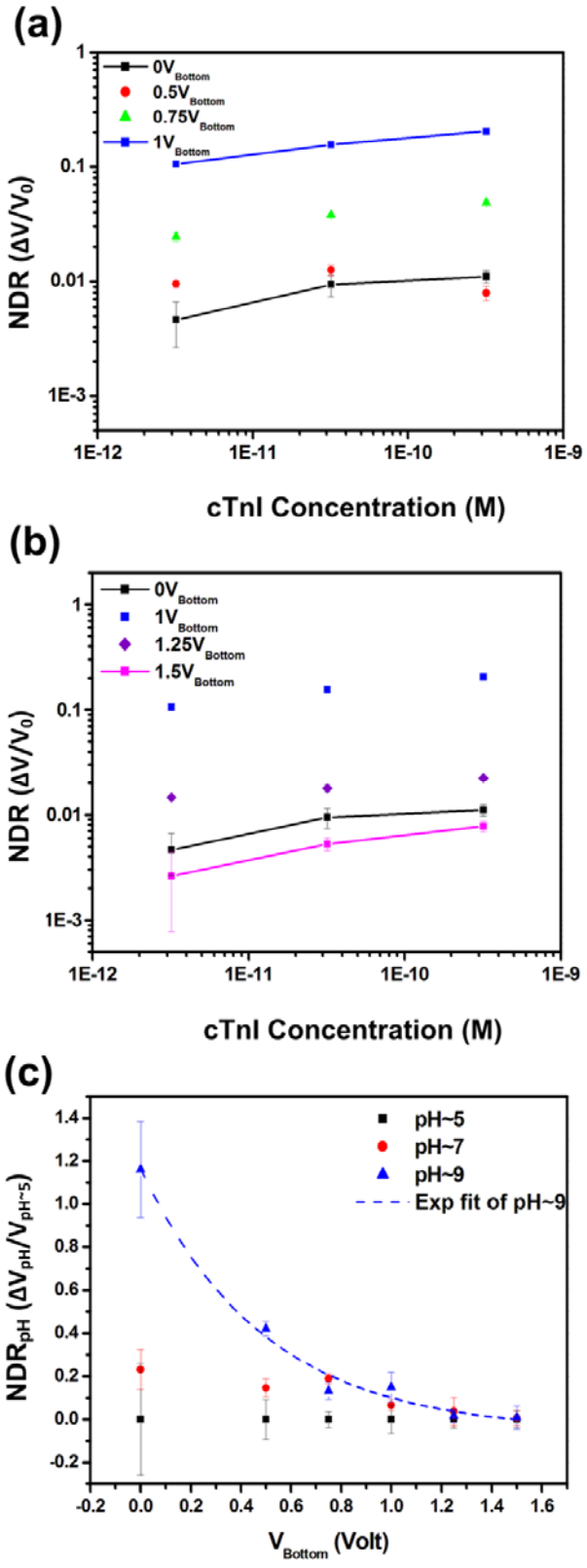
(a)
0V Bottom
0.5V Bottom
0.75V Bottom
1V Bottom
NDR (ΔV/V0)
1
0.1
0.01
1E-3
1E-12
1E-11
1E-10
1E-9
cTnI Concentration (M)
(b)
0V Bottom
1V Bottom
1.25V Bottom
1.5V Bottom
NDR (ΔV/V0)
1
0.1
0.01
1E-3
1E-12
1E-11
1E-10
1E-9
cTnI Concentration (M)
(c)
pH~5
pH~7
pH~9
Exp fit of pH~9
NDRpH (ΔVpH/VpH~5)
1.4
1.2
1.0
0.8
0.6
0.4
0.2
0.0
-0.2
-0.2
0.0
0.2
0.4
0.6
0.8
1.0
1.2
1.4
1.6
VBottom (Volt)

Fig. 4

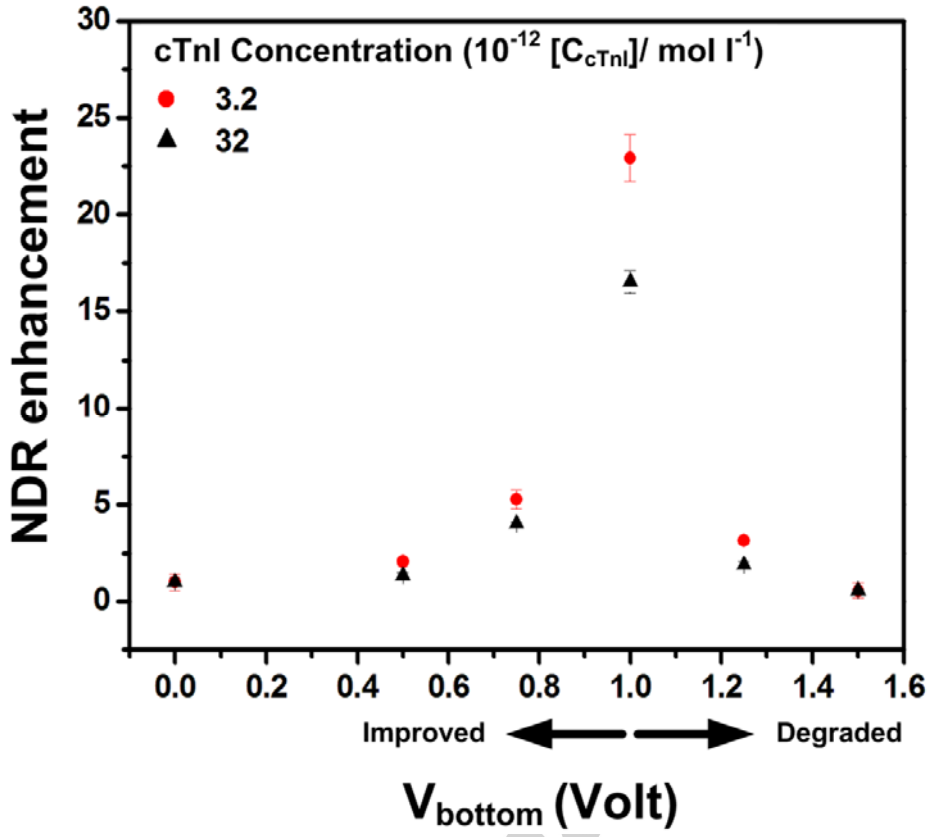

Fig. 5

Table 1.

C_{cTnI} (10^{-12}[C_{cTnI}]/M)	0 V_{bottom}	0.5 V_{bottom}	0.75 V_{bottom}	1 V_{bottom}	1.25 V_{bottom}	1.5 V_{bottom}
3.2	1.0 ± 0.4	2.1 ± 0.2	5.3 ±0.5	22.9 ± 1.2	3.1 ± 0.2	0.6 ± 0.4
32	1.0 ± 0.2	1.3 ± 0.2	4 ±0.1	16.5 ± 0.6	1.9 ± 0.2	0.6 ± 0.1

A device design of CMOS integrated poly-silicon biosensor-on-chip to enhance cardiac troponin-I detection performance in serum samples

Pei-Wen Yen[1], Che-Wei Huang[2], Yu-Jie Huang[2], Min-Cheng Chen[3], Hsin-Hao Liao[4], Shey-Shi Lu[2], and Chih-Ting Lin[1,2,*]

[1]Graduate Institute of Biomedical Electronics and Bioinformatics, National Taiwan University, Taipei, Taiwan

[2] Graduate Institute of Electronics Engineering, National Taiwan University, Taipei, Taiwan

[3]National Nano Device Laboratory, National Applied Research Laboratories, Hsinchu, Taiwan

[4]National Chip Implementation Center, National Applied Research Laboratories, Hsinchu, Taiwan

*Corresponding author. Tel: +886 2 33669603, Fax: +886 2 23681679 Email: timlin@ntu.edu.tw

Highlights

- Poly-silicon nanowire biosening system-on-chip is implemented
- Bottom-gate design improves poly-SiNW biosensor response in serum samples
- Figure-of-merit of applied bottom-gate potential is characterized